NAVAL POSTGRADUATE SCHOOL
MONTEREY, CALIFORNIA

THESIS

EFFECTS OF TOWED-DECOYS AGAINST AN ANTI-AIR MISSILE WITH A MONOPULSE SEEKER

by

Jia-Hsin Yeh

September 1995

Thesis Advisor: D. Curtis Schleher

19960220 004

DTIC QUALITY INSPECTED 1

REPORT DOCUMENTATION PAGE

Form Approved OMB No. 0704-0188

1. AGENCY USE ONLY *(Leave blank)*	2. REPORT DATE September 1995	3. REPORT TYPE AND DATES COVERED Master's Thesis	

4. TITLE AND SUBTITLE Effects of Towed-Decoys Against An Anti-Air Missile with A Monopulse Seeker	5. FUNDING NUMBERS
6. AUTHOR(S) Jia-Hsin Yeh	

7. PERFORMING ORGANIZATION NAME(S) AND ADDRESS(ES) Naval Postgraduate School Monterey CA 93943-5000	8. PERFORMING ORGANIZATION REPORT NUMBER
9. SPONSORING/MONITORING AGENCY NAME(S) AND ADDRESS(ES)	10. SPONSORING/MONITORING AGENCY REPORT NUMBER

11. SUPPLEMENTARY NOTES The views expressed in this thesis are those of the author and do not reflect the official policy or position of the Department of Defense or the U.S. Government.

12a. DISTRIBUTION/AVAILABILITY STATEMENT Approved for public release; distribution is unlimited.	12b. DISTRIBUTION CODE

13. ABSTRACT *(maximum 200 words)*

This thesis evaluates the protection provided by towed-decoys deployed by an aircraft during an engagement against an anti-air missile equipped with a monopulse seeker. The research emphasizes the use of passive decoys. Many of the operational paramenters required before the deployment of towed-decoy are investigated, including the strength of reflection, the tether length, the direction of release, under different missile incoming directions.

This thesis evaluated two reflection cases. One is for both target and decoy being point reflectors. The other is for an extended target and a point reflected decoy. The protection envelopes for different engagement scenarios of each reflection case is obtained.

14. SUBJECT TERMS ECM, monopulse, towed-decoy, missiles	15. NUMBER OF PAGES 46
	16. PRICE CODE

17. SECURITY CLASSIFICATION OF REPORT Unclassified	18. SECURITY CLASSIFICATION OF THIS PAGE Unclassified	19. SECURITY CLASSIFICATION OF ABSTRACT Unclassified	20. LIMITATION OF ABSTRACT UL

NSN 7540-01-280-5500

Standard Form 298 (Rev. 2-89)
Prescribed by ANSI Std. 239-18 298-102

EFFECTS OF TOWED-DECOYS AGAINST AN ANTI-AIR MISSILE WITH A MONOPULSE SEEKER

Jia-Hsin Yeh

Captain, Taiwan, R. O. C., Air Force
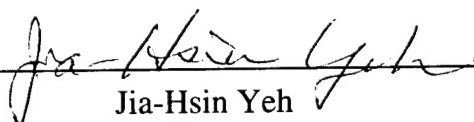
B.S., Chung-Cheng Institute of Technology, 1988

Submitted in partial fulfillment

of the requirements for the degree of

MASTER OF SCIENCE IN SYSTEM ENGINEERING
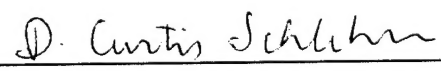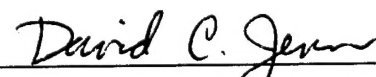
from the

NAVAL POSTGRADUATE SCHOOL
September 1995

Author: _____

Jia-Hsin Yeh

Approved by: _____

D. Curtis Schleher, Thesis Advisor

_____

David Jenn, Second Reader

_____

Fred Levien, Chairman

Electronic Warfare Academic Groups

ABSTRACT

This thesis evaluates the protection provided by towed-decoys deployed by an aircraft during an engagement against an anti-air missile equipped with a monopulse seeker. The research emphasizes the use of passive decoys. Many of the operational parameters required before the deployment of a towed-decoy are investigated, including the strength of reflection, the tether length, and the direction of release, under different missile incoming directions.

The thesis evaluates two reflection cases. One is for both the target and the decoy being point reflectors. The other is for an extended target and a point reflected decoy. The protection envelopes for different engagement scenarios of each reflection case is obtained.

TABLE OF CONTENTS

LIST OF FIGURES

I. INTRODUCTION

Monopulse, or simultaneous-lobing tracking, obtains an angle error estimate from a single pulse return. Unlike sequential-lobing systems, monopulse radar does not require a long integration time or demodulation process, resulting in an immunity to noise jamming effects. This inherent ECCM against many on-board jamming techniques explains why so many missiles have adopted monopulse trackers for their guidance seekers. Also many sequential-lobing trackers have been modified using monopulse techniques to reduce their vulnerability to jamming.

From a self-protection point of view, a fighter pilot needs an effective ECM method to counter missiles with monopulse seekers. Since on-board equipment has limited effectiveness, expendables, especially decoys, become a reasonable choice. However, modern missiles can distinguish the difference in Doppler frequencies between aircraft and conventionally free-falling decoys using MTI techniques leading to a preference for towed-decoys.

An initial evaluation leads to the conclusion that a towed-decoy provides a counter to a monopulse seeker. However, its effectiveness is always in question. A critical question concerns the protection it can provide under different missile attack angles. Further, there are some parameters that must be decided prior to deployment of a decoy. For example, the length of the tether line, the strength of the reflection from the decoy, and the direction of release, to name just a few. This thesis investigates all the above questions using a computer-based simulation based upon the scenario shown in Figure 1.
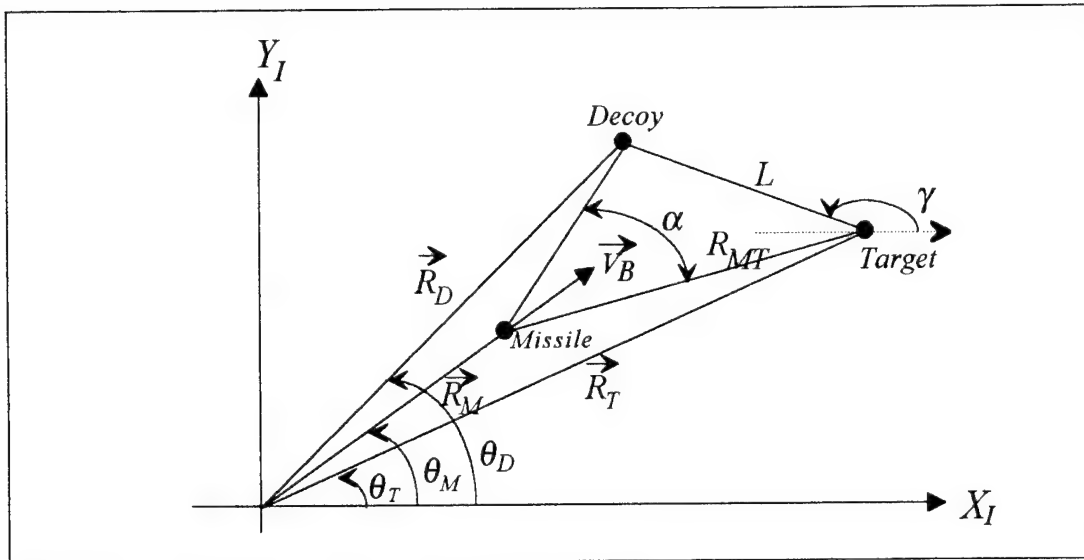
Figure 1. Scenario Geometry

Description of Parameters:

X_I, Y_I = Inertial reference axes

R_M, R_T, R_D = Missile, target, and decoy position vectors with respect to inertial frame

V_B = Missile velocity vector

R_{MT} = Position vector of missile to target

R_{MD} = Position vector of missile to decoy

L = Tether line length

γ = Decoy deployment angle

α = Subtended angle between target and decoy

θ_T, θ_M, θ_D = Orientations of target, missile, and decoy with respect to inertial frame

2

II. MONOPULSE ANGLE ESTIMATION

There are several types of monopulse angle sensors that are categorized by their sensing and detection methods. The most commonly used and preferred one is the amplitude sensing, sum-difference detection type. This is the kind of sensor investigated in this thesis.

The general radar seeker model is shown in Figure 2.
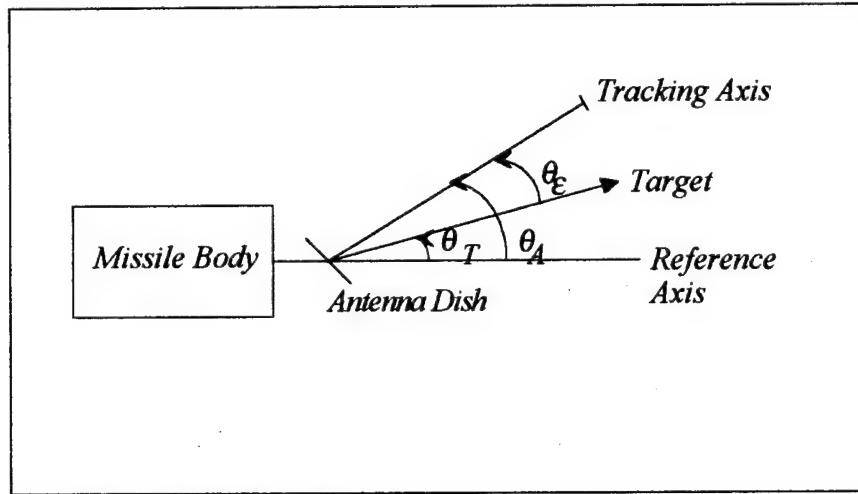
Figure 2. Radar Tracking Axes

In Figure 2, the reference axis is the missile body roll axis while θ_ε is the angular tracking error defined as the angle between the seeker tracking axis and the line-of-sight. Assuming Gaussian distributed antenna patterns:

$$G(\theta) = G_0 \exp\{-k(\frac{\theta-\theta_S}{\theta_3})^2\} \tag{1}$$

where, θ_3 is the antenna beamwidth, θ_S is the squint angle, and $k = 2.776$, results in received voltages given by:

3

$$v_1 = SG_0 \exp\left\{-k\left(\frac{\theta-\theta_S}{\theta_3}\right)^2\right\} \quad \text{and} \quad v_2 = SG_0 \exp\left\{-k\left(\frac{\theta+\theta_S}{\theta_3}\right)^2\right\} \tag{2}$$

and S is the strength of the target skin return. The receiving patterns are shown in Figure 3-a.
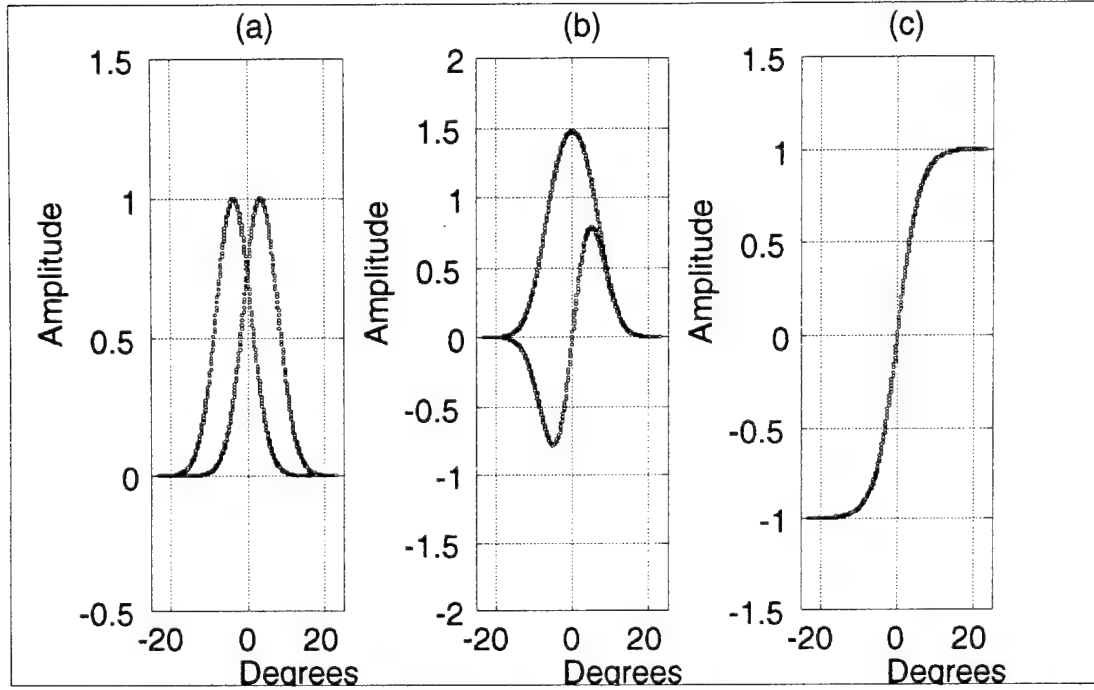
Figure 3-a. Gaussian Antenna Patterns

      3-b. Sum Beam and Difference Beam Patterns

      3-c. Error Voltage

If the IF gains of both sum and difference channels are matched (i.e., $K_\Sigma = K_\Delta$), then, the outputs of the sum and difference channels are:

$$\Sigma = v_1 + v_2 \quad \text{and} \quad \Delta = v_1 - v_2 \tag{3}$$

Now, the output of the phase detector is the error voltage, ε,

$$\varepsilon = \text{Real}\{V_\Delta/V_\Sigma\} \tag{4}$$

The error voltage, or monopulse ratio, is proportional to the angular tracking error, θ_ε. It serves as an input to the seeker angle servo which acts to lock the tracking axis onto the target by nullifying the tracking error. The sum and difference receiving channels signals and resulting error voltage are shown in Figure 3-b and 3-c. The whole process is illustrated in the block diagram of Figure 4.
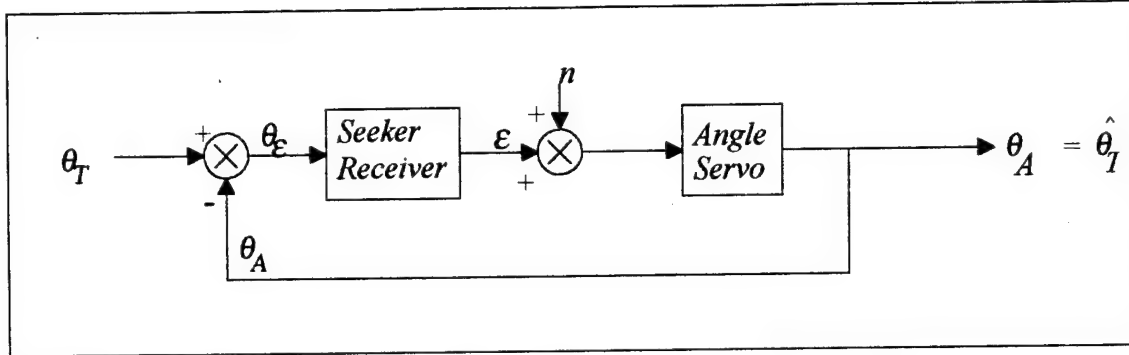
Figure 4. Angle Tracking Block Diagram

As shown in Eq. 4, the error voltage is the real part of the normalized (with respect to the sum signal) difference signal. No matter how strong an on-board jamming signal is, it is always spatially coincident with the target signal. Thus, the error voltage does not change with on-board jamming. That is why an off-board source is needed to perform angular deception against a monopulse seeker.

Double-Source Problem

For a double-source geometry shown as Figure 1 of Chapter I, the received voltage from each beam is:

$$v_1 = v_{T_1} + v_{D_1} = SG_0 \exp\left\{-k\left(\frac{\theta_T - \theta_S}{\theta_3}\right)^2\right\} + JG_0 \exp\left\{-k\left(\frac{\theta_D + \theta_S}{\theta_3}\right)^2\right\} e^{j\psi} \qquad (5)$$

$$v_2 = v_{T_2} + v_{D_2} = SG_0 \exp\left\{-k\left(\frac{\theta_T - \theta_S}{\theta_3}\right)^2\right\} + JG_0 \exp\left\{-k\left(\frac{\theta_D + \theta_S}{\theta_3}\right)^2\right\} e^{j\psi} \qquad (6)$$

where ψ is the phase relation between target and decoy returns. This is given by:

$$\psi = 2\pi\left(\frac{\delta L}{\lambda}\right) \tag{7}$$

where δL is the path difference. Then, the sum and difference channels have voltages:

$$\Sigma = v_1 + v_2 \quad \text{and} \quad \Delta = v_1 - v_2 \tag{8}$$

Again, the indicated angle can be derived from the error voltage:

$$\varepsilon = \text{Real}\{\Delta/\Sigma\} \tag{9}$$

The introduction of the second source results in distortion of the real part of the monopulse ratio. The tracking axis does not point at the target any longer. Instead, it generally tracks the power centroid of the two sources until they can be resolved. When the seeker starts to resolve the two sources, it tracks the stronger source. The resolving condition occurs when the subtended angle is greater than the seeker's beamwidth; this distance is:

$$s \leq \left(\frac{L}{2}\right)/\tan\left(\frac{\theta_3}{2}\right) = L/(2\tan\frac{\theta_3}{2}) \tag{10}$$

III. SIMULATION ARCHITECTURES

The simulation is explained using the block diagram shown in Figure 5. Using missile/target geometry, the aspect angles of the target and decoy are provided as inputs to the seeker model. This allows the tracking error to be estimated. The seeker's tracking axis is pointed at the line-of-sight between the missile and the composite target/decoy return. The lateral acceleration required to turn the missile is simply

$$a_{CMD} = N \bullet \hat{\theta}_A \bullet V_B \qquad (11)$$

where N is the navigation constant. This steering command goes into the actuator model to drive the deflection of the missile control surface and change the missile attitude towards the target.

To simplify the analysis several assumptions are made. First, the simulation is limited to an azimuth-plane only rather than to a three-dimensional geometry. This simplifies the simulation and allows results to be obtained. Second, the missile dynamics are assumed to have a 1 Hz response while the actuator is limited to 10G acceleration. Third, the monopulse seeker uses amplitude sensing with sum-difference detection. Further it is assumed that the seeker gimbal has 20 Hz response with angle limits of ±45°. This high dynamic seeker gimbal performance avoids dynamic coupling with the missile. The antenna beamwidth (θ_3) is approximately 11.5°.

The measure of effectiveness used is the miss distance (i.e., the range between missile and target). It is set such that the missile will detonate if it is within 5 meters range to the target (either the aircraft or the decoy). There are times when the missile does not

7

impact on either of the targets. Under these circumstances, the miss distance is recorded as the shortest missile-to-aircraft range (i.e., minimum R_{MT}, during the whole simulation). Therefore, these recorded miss distances become the minimum protection envelope that the decoy can provide.
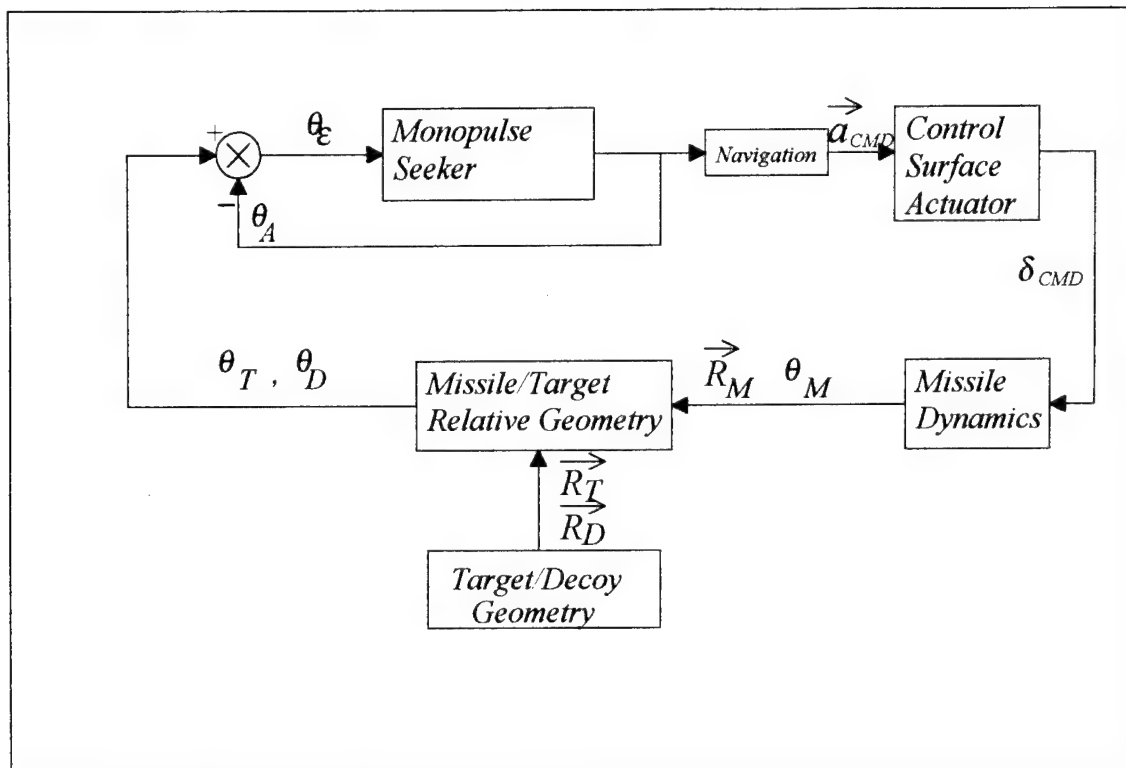
Figure 5. Simulation Block Diagram

IV. DECOY EFFECTS FOR A POINT REFLECTION TARGET

A.   LAYOUT GEOMETRY

Before discussing the effects of different decoy deployment conditions, the reference coordinate system is first defined. There are two angles of interest in this thesis. One is the decoy deployment angle while the other is the initial missile attack angle. Let the angle β be defined as shown in Figure 6. In Figure 6-a, $\beta = \gamma$, is used to analyze decoy deployment angle effects; whereas in Figure 6-b, $\beta = \theta_M$, is used to analyze initial missile attack direction effects. The missile/target engagement situation can be categorized as:

(i). For $\beta = 45° \sim 135°$ or $-45° \sim -135°$, the target aircraft undergoes a side-attack situation.

(ii). For $\beta = 135° \sim 225°$, the target aircraft undergoes a head-on attack situation.

(iii). For other β, the target aircraft undergoes a tail-pursuit situation.
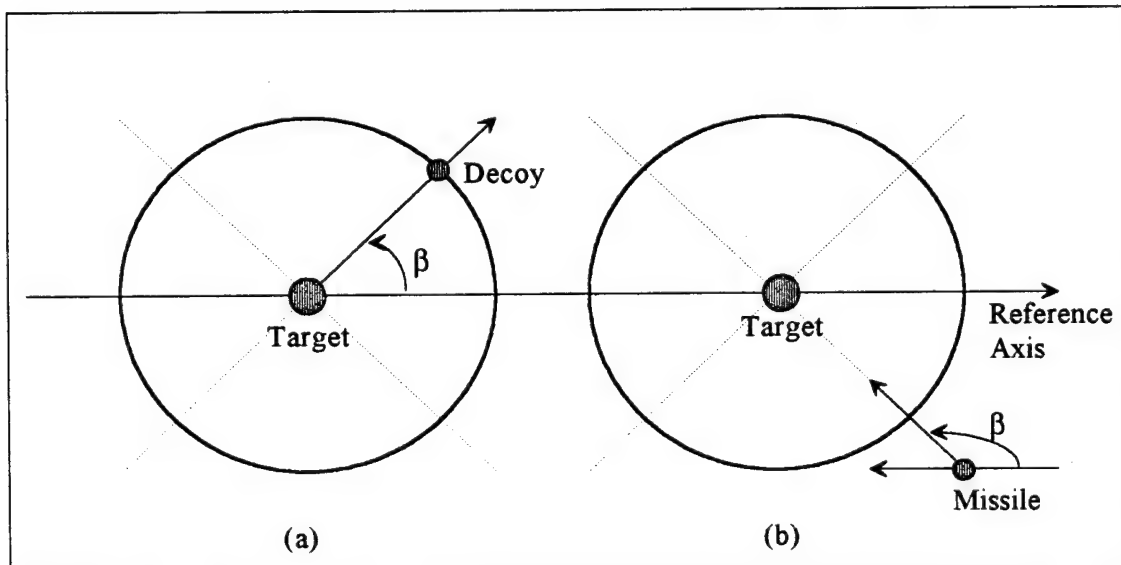
Figure 6. Layout Geometry

B.   EFFECTS OF REFLECTION RATIO

Figure 7 shows the effects on miss distance resulting from three different tether lengths as a function of the relative decoy to target ratios. It shows that the longer the tether line is, the higher the reflection ratio (σ_D/σ_T) required to effectively capture the seeker's angle tracking loop. Moreover, when the reflection ratio reached 1.5, the effects on miss distance stabilized. At that point, the missile will home onto the decoy.
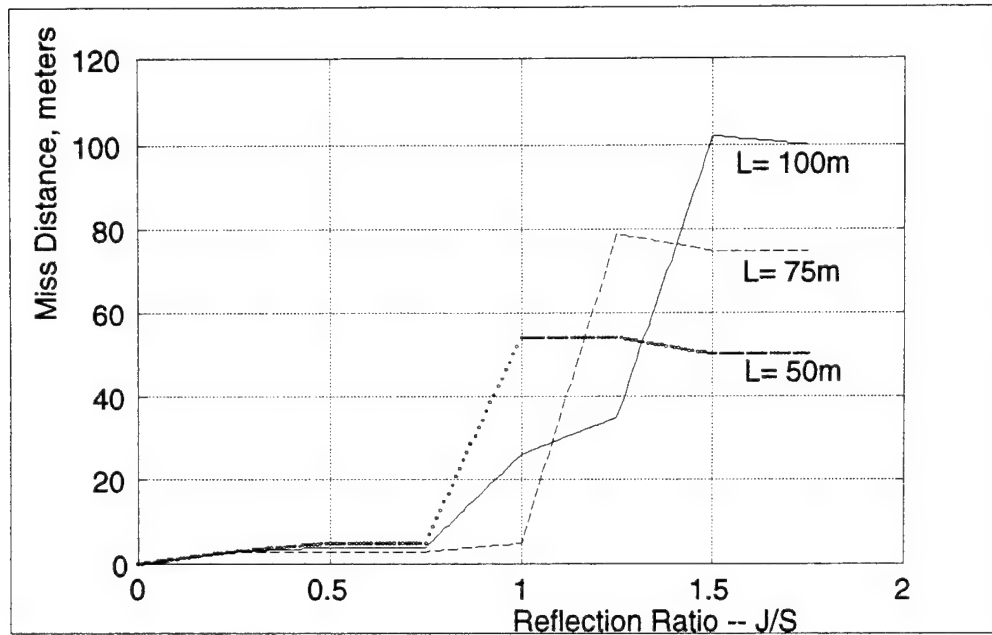
Figure 7. Effect of Reflection Ratio on Miss Distance,

Decoy at 150° and Missile from 180°

Figure 8 shows a side-attack situation. The decoy is more effective with this operation, and $\sigma_D/\sigma_T = 1.25$ is sufficient to protect the aircraft.
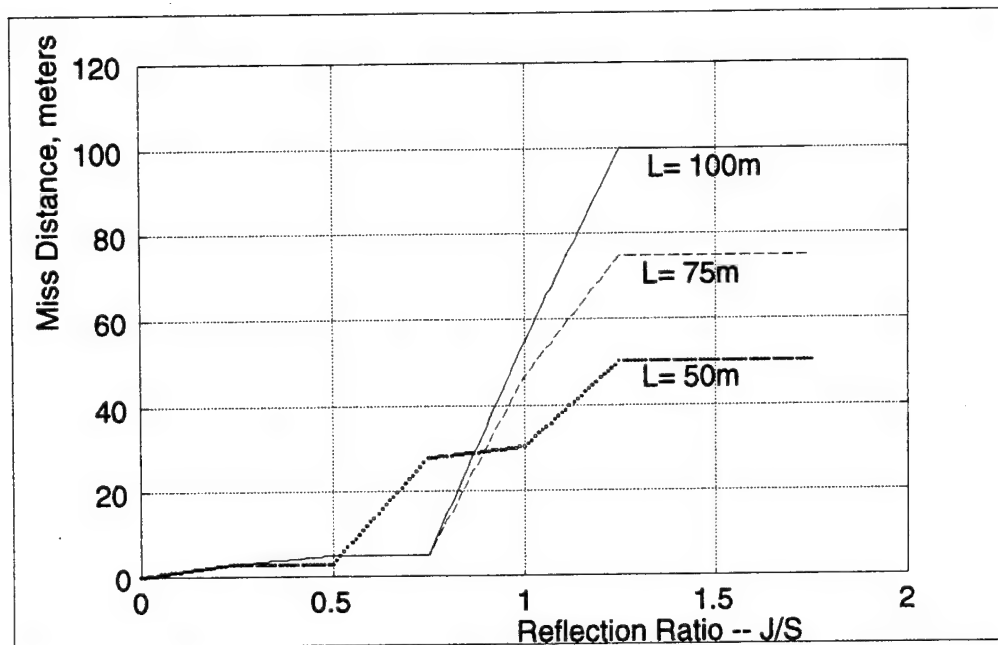
Figure 8. Effect of Reflection Ratio on Miss Distance,

Decoy at 180° and Missile from 90°

C. CHANGE OF MISS DISTANCES DUE TO DIFFERENT MISSILE ATTACK ANGLES

Figure 9 shows that for a reflection ratio of 1 with the decoy deployed at 180°, the protection from tail-approaching missiles stays almost constant independent of tether lengths. The protection from side-attack missile reduces as the tether length increases. Note also that when the tether length increases, null regions become more obvious and the protection regions get smaller. This, again, shows that for longer tether lengths, a higher reflection ratio is required to capture the angle-tracking loop of the seeker.
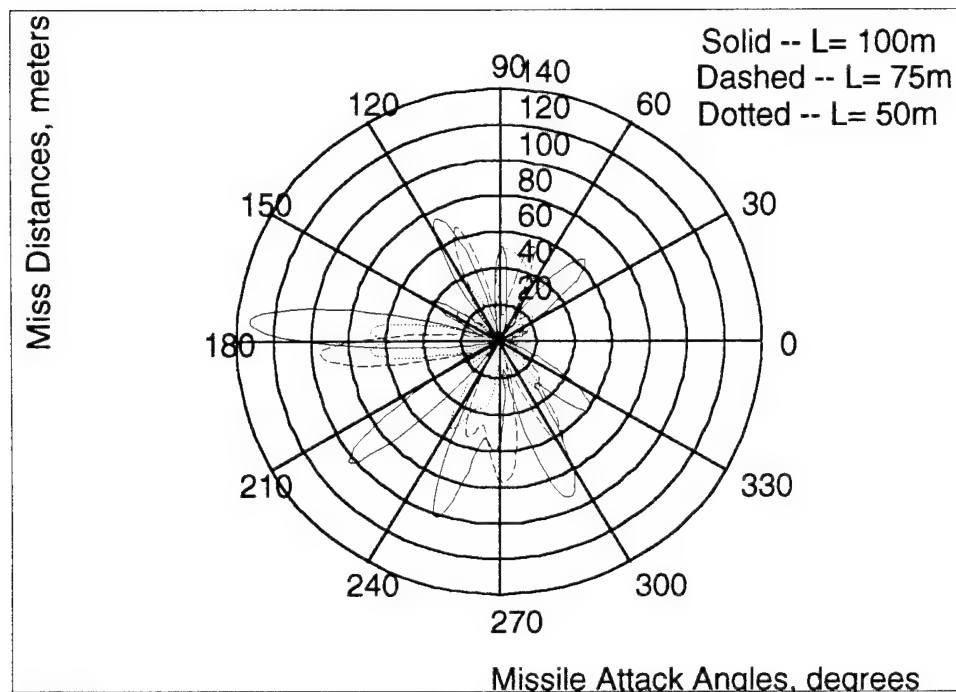
Figure 9. Protection Envelope of Different Missile Attack Angles

for $\sigma_D/\sigma_T = 1$

This point is illustrated by Figure 10 where for a reflection ratio of 1.5 a wider protection envelope is provided. Effective protection is provided when encountering a tail-attack missile, with the decoy parameters set to $\sigma_D/\sigma_T = 1.5$ and L = 50m; whereas when a side-attack missile is encountered, $\sigma_D/\sigma_T = 1.5$ and L = 75m is recommended. The reason that L = 100m isn't preferred is due to the many nulls in the protection pattern, which means that in some cases the missile may lock-on to the aircraft. Also, long tether lengths are not convenient if evasive maneuvers are required.

12
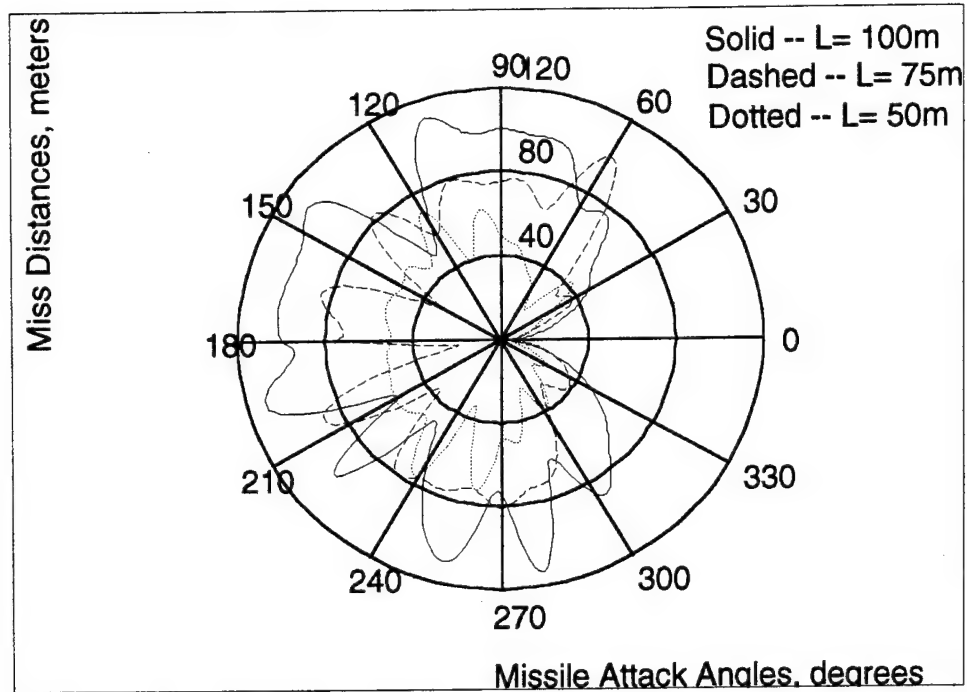
Figure 10. Protection Envelope of Different Missile Attack Angles

for $\sigma_D/\sigma_T = 1.5$

D. CHANGE OF MISS DISTANCES DUE TO DIFFERENT DECOY DEPLOYMENT ANGLES

The following discusses the parameters associated with decoy deployment for $\sigma_D/\sigma_T = 1.5$ with the missile attacking from 180°. Figure 11 shows that different tether lengths can provide maximum protection if the decoy is deployed perpendicular to the incoming direction of the missile. However, this is not operationally feasible under practical flight conditions. Nevertheless, comparison of Figure 11 with Figure 10 shows one thing in common. That is, decoy deployment has the most affect on side-attacking missiles independent of the tether length. Actually, the longer the length is, the better the protection once the reflection ratio has reached its effectiveness equilibrium.

13
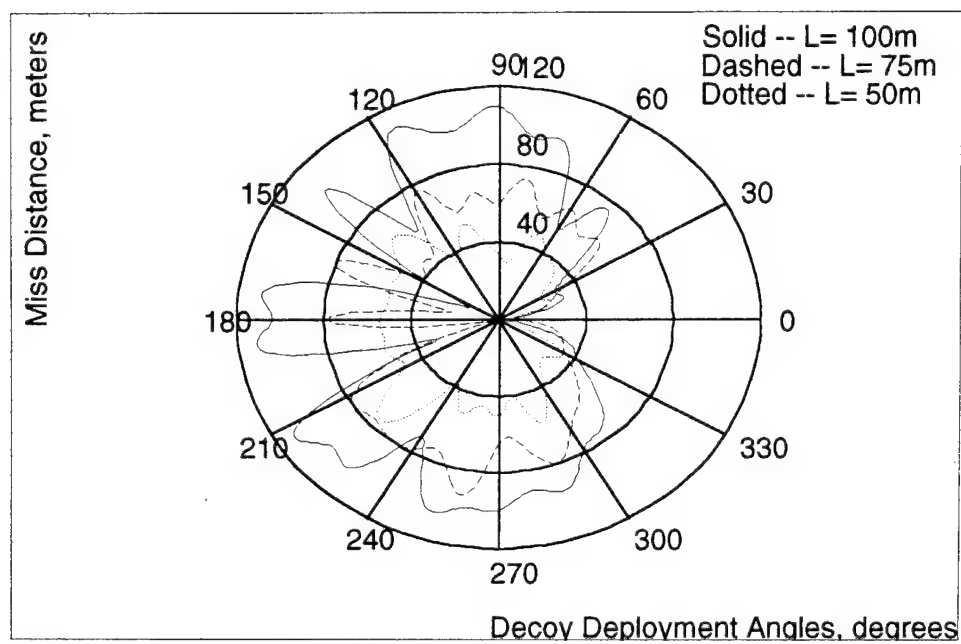
Figure 11. Protection Envelope of Different Decoy Deployment Angles

for $\sigma_D/\sigma_T = 1.5$

V. DECOY EFFECTS FOR AN EXTENDED TARGET

For most practical situations, the target is not a point reflection source. Rather the target is extended and composed of many scatters. For simplification, the target aircraft will be represented as a 10 meters long (L = 10m), 1 meter radius (a = 1m) cylinder. Then, the monostatic reflection is given by [Ref. 1]:

$$\sigma = kaL^2 \left| \cos\theta_i \frac{\sin(kL\sin\theta_i)}{kL/\sin\theta_i} \right|^2 \tag{12}$$

where θ_i is the angle of incidence from the broadside in a plane containing the cylinder axis, and $k = 2\pi/\lambda$, where $\lambda = 0.03$m. This target reflection is shown in Figure 12 where $\sigma_{max} = 5.45$ m^2 and $<\sigma^2>_{av} = 4.56$ m^2. For the discussion in this chapter, the reflection ratio is defined as $\sigma_D/\max(\sigma_T)$.
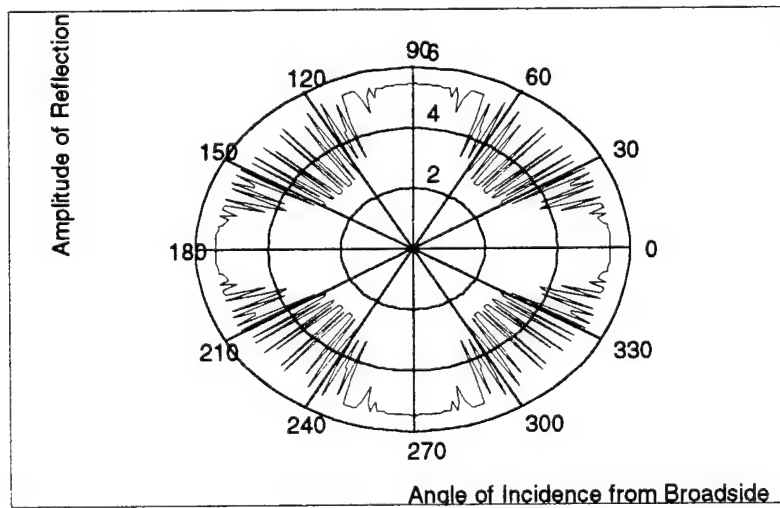
Figure 12. Extended Target Reflection

A. EFFECTS OF REFLECTION RATIO

As shown in Figure 13, the effects on miss distance from a change in reflection ratio achieved stabilization when $\sigma_D/\max(\sigma_T) = 1.5$ for a side-attack situation (missile from 90°) and decoy at 180°. The result is consistent with the point target case. It also shows that when $\sigma_D/\max(\sigma_T) = 1$, it protects the target for each tether length. Thus, the reflection required for the decoy in operation should not be less than that of the target it protects.
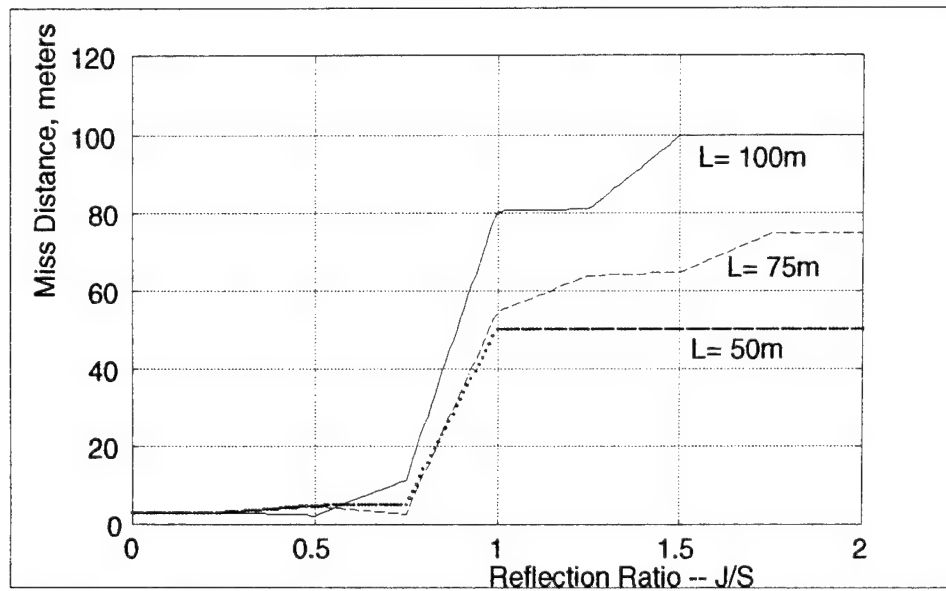
Figure 13. Effect of Reflection Ratio on Miss Distance for Extended Target

B. CHANGE OF MISS DISTANCE DUE TO DIFFERENT MISSILE ATTACK ANGLES

Figure 14 shows that for a $\sigma_D/\max(\sigma_T)$ ratio of 1.5 and the decoy at 180°, the protection envelope provided by the decoy is almost the same as Figure 10. Still, it provides maximum protection for a side-attack situation, i.e., when the decoy is deployed

perpendicular to the incoming direction of the missile. Since the result is obtained when the reflection of the decoy has reached its stabilized condition, it is safe to say that the towed-decoy is a very effective countermeasure against a monopulse seeker missile.
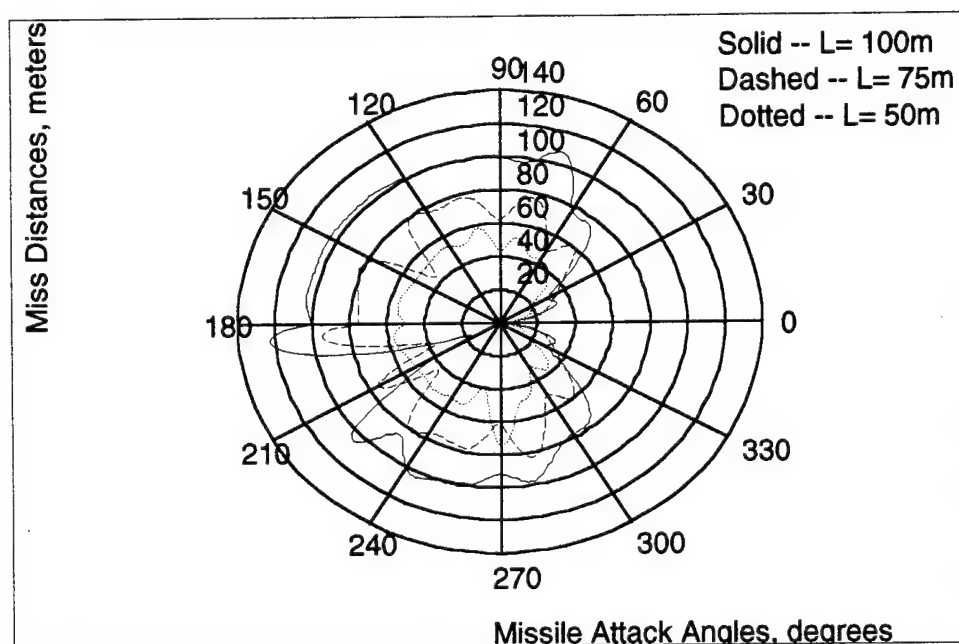
Figure 14. Protection Envelope of Different Missile Attack Angles for Extended Target

C. CHANGE OF MISS DISTANCE DUE TO DIFFERENT DECOY DEPLOYMENT ANGLES

Figure 15 shows the protection envelope when $\sigma_D/\max(\sigma_T)$ is 1.5 with the missile approaching from 180°. Compared with the protection envelope in Figure 11, some of the notches have disappeared for longer tether lengths. Also, the protection envelope grows as the tether length increases. This results in the decoy having a wider deployment choice when the tether length of the decoy is longer.

Figure 15. Protection Envelope of Different Decoy Deployment Angles for Extended Target

VI. CONCLUSIONS

This thesis has investigated two kinds of target/decoy reflection conditions. One is when both the target and decoy are point reflectors, while the other is for an extended target while the decoy remains 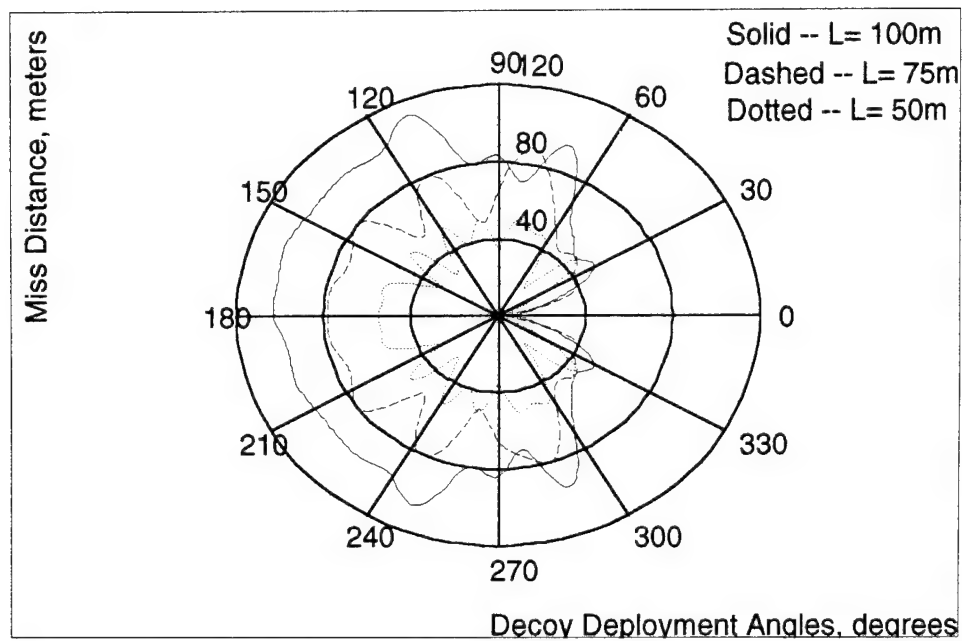as a point reflector. Three different deployment cases are considered: (1) the change of the reflection from the decoy, (2) the change of direction of release, and (3) the change of initial missile incoming direction, under different tether lengths.

The result has shown that a towed-decoy is indeed an effective countermeasure against monopulse seeker missiles. The operational parameters have the following characteristics:

- The decoy starts to take effect when its reflection is stronger than the protected target. Longer tether length requires stronger reflections to reach stabilization than shorter length. The reflection ratio required for stabilization is about 0.1 for every 10 meters length increment. When the reflection ratio reached 1.5, the missile will home directly onto the decoy.

- For both target reflection cases, the decoy is most effective when it is deployed toward, or perpendicular, to the missile incoming direction. However, for the extended target case, the decoy has a wider choice of deployment regions than the constant target case.

- The decoy provides a very wide protection region for any missile attack angle except for head-on situations where no protection is provided. There are notches in protection envelopes. However, for longer tether lengths, the notches become less pronounced which indicates that a longer tether length is preferred. If we take maneuverability into account, tether lengths should be less than 100 meters but at least twice as long as the missile's lethal range.

19

VII. FUTURE STUDIES

Towed-decoys have attracted the attention of many EW engineers and companies. According to [Ref. 2], "Towed decoys top the RF development list." This thesis provides a preliminary insight regarding the operational deployment parameters required for the use of towed decoys. There is still additional work required beyond that covered in this thesis to ensure effective use of towed decoys. The following describes some of this work:

- In this thesis we assume a fully deployed towed decoy. This results in the missile viewing the decoy at its fully stabilized condition (i.e., full length, full strength of reflection). The discrimination conditions which result when a single source transitions to a double source should be further studied.

- The imaginary part induced (see Eqs. 5 and 6) from the introduction of the second source can serve as a warning that the seeker has been jammed. This possible countermeasure from the seeker's point of view can be studied as a possible ECCM against towed decoys.

- This thesis does not consider the effects of target glint and scintillation. They may be major factors in the determination of the seeker's resolving capability before lock-on. These effects need further exploration.

- Target maneuvers which change the relative bearings between the target and the decoy require further investigation to determine their effects on the protection envelopes.

21

APPENDIX A - THESIS MAIN PROGRAM

```
ang_init = input('Missile's Initial Firing Angle = ');
R0 = 4000;
RX0 = 5000;
RY0 = 2000;
tf = input('End Time = ');
md = input('End Game Requirement = ');
TL = input('Towed-line Length = ');
Dploy1 = input('Decoy Deployment Angle = ');
RCS = input('RCS Ratio (RCSd/RCSt)= ');
RCSmax= 5.4562;      % Target  Maximum RCS
RCSd= RCS.*RCSmax;

% Angle Transformation
d2r = pi/180;
r2d = 180/pi;

% Missile Initial Position
RX_init = RX0-R0*cos(ang_init*d2r);
RY_init = RY0-R0*sin(ang_init*d2r);

% Missile Parameters
mass = 150;
Izz = 150;
PPN = 4;         % PPN Constant

% Initial Run for Initial Conditions
n=1;
step(n) = .05;
trun(n) = (n-1).*step(n);
psim(n)=ang_init*d2r;
VMXI(n) = 250*cos(psim(n));
VMYI(n) = 250*sin(psim(n));
VM(n) = sqrt(VMXI(n).^2+VMYI(n).^2);
RMXI(n) = RX_init;
RMYI(n) = RY_init;
RM(n) = sqrt(RMXI(n).^2+RMYI(n).^2);
I2B0 = tml(psim(n));            % Transformation Matrix
```

```matlab
[VMXB(n),VMYB(n)] = i2btran(VMXI(n),VMYI(n),I2B0);
VB(n) = sqrt(VMXB(n).^2+VMYB(n).^2);
AMXB(n) = 0;
AMYB(n) = 0;
[AMXI(n),AMYI(n)] = b2itran(AMXB(n),AMYB(n),I2B0);
RDOT(n) = 0;
r(n) = 0;
beta(n) = aoa3(VMXB(n),VMYB(n));
delr(n) = 0;
DR(n) = 0;
CFX(n) = 0;
CFY(n) = 0;
CMZ(n) = 0;
FX(n) = 0;
FY(n) = 0;
N(n) = 0;

% Target Parameters
VTXI = 0;
VTYI = 0;
RTXI(n) = RX0;
RTYI(n) = RY0;
RT(n) = sqrt(RTXI(n).^2+RTYI(n).^2);

% Decoy Parameters
dploy = dploy1.*d2r;
TDXI = TL.*cos(dploy);
TDYI = TL.*sin(dploy);

% Missile/Target Relative Geometry
RMTX(n) = RTXI(n)-RMXI(n);
RMTY(n) = RTYI(n)-RMYI(n);
RMT(n) = sqrt(RMTX(n).^2+RMTY(n).^2);
[mtbx(n),mtby(n)] = i2btran(RMTX(n),RMTY(n),I2B0);
psilos(n) = atan2(mtby(n),mtbx(n));
psilosd(n) = psilos(n)*r2d;
RCSt(n) = raylei(psilos(n));

% Missile/Target/Decoy Relative Geometry
RDXI(n) = RTXI(n)+TDXI;
RDYI(n) = RTYI(n)+TDYI;
MDXI(n) = RDXI(n)-RMXI(n);
MDYI(n) = RDYI(n)-RMYI(n);
```

```
RMD(n) = sqrt(MDXI(n).^2+MDYI(n).^2);
[mdbx(n),mdby(n)] = i2btran(MDXI(n),MDYI(n),I2B0);
psid(n) = atan2(mdby(n),mdbx(n));
psidd(n) = psid(n)*r2d;
disc(n) = max(RMT(n),RMD(n));
RXI(n) = RMTX(n)+.5.*TDXI;
RYI(n) = RMTY(n)+.5.*TDYI;
RR(n) = sqrt(RXI(n).^2+RYI(n).^2);
subang(n) = acos( (RMT(n).^2+RMD(n).^2-TL^2)./(2*RMT(n)*RMD(n)) );
dL(n) = RMD(n)-RMT(n).*cos(subang1(n));
dphase(n) = rem(4.*pi.*dL(n)./(.03),2*pi);
VMTX(n) = VTXI-VMXI(n);
VMTY(n) = VTYI-VMYI(n);

% for Seeker
skrang(n) = 0;
sd(n) = 0;
acmd(n) = 0;
ve(n) = 0;
Vsum(n) = 0;
Vdel(n) = 0;
Pest(n) = 0;

% Start Running
while trun(n) <= tf
n=n+1;
count = n;
step(n) = ftime(disc(n-1),TL);
trun(n) = trun(n-1)+step(n);

[skrang(n),sd(n),ve(n),Vsum(n),Vdel(n),Pest(n)]=yskr(psilos(n-1),skrang(n-1),sd(n-1),...
                flag,step(n),RCSt(n-1),RCSd,subang(n-1),dphase(n-1),psid(n-1));
acmd(n) = skrang(n)*PPN*VB(n-1);
delr(n) = fin(acmd(n),delr(n-1),count);
DR(n) = delr(n)*r2d;
[CFX(n),CFY(n),CMZ(n)] = aero(beta(n-1),delr(n),VB(n-1),flag,r(n-1),trun(n));
[FX(n),FY(n),N(n)] = fm22(CFX(n),CFY(n),CMZ(n),flag,trun(n),VB(n-1));
AMXB(n) = FX(n)/mass;
AMYB(n) = FY(n)/mass;
RDOT(n) = N(n)/Izz;
r(n) = intgr(RDOT(n-1),RDOT(n),r(n-1),flag,step(n));
I2B = tm1(psim(n-1));
[AMXI(n),AMYI(n)] = b2itran(AMXB(n),AMYB(n),I2B);
```

```
VMXI(n) = intgr(AMXI(n-1),AMXI(n),VMXI(n-1),flag,step(n));
VMYI(n) = intgr(AMYI(n-1),AMYI(n),VMYI(n-1),flag,step(n));
psim(n) = atan2(VMYI(n),VMXI(n));
[VMXB(n),VMYB(n)] = i2btran(VMXI(n),VMYI(n),I2B);
VB(n) = sqrt(VMXB(n).^2+VMYB(n).^2);
RMXI(n) = intgr(VMXI(n-1),VMXI(n),RMXI(n-1),flag,step(n));
RMYI(n) = intgr(VMYI(n-1),VMYI(n),RMYI(n-1),flag,step(n));
RM(n) = sqrt(RMXI(n).^2+RMYI(n).^2);
beta(n) = aoa3(VMXB(n),VMYB(n));
RTXI(n) = RX0+VTXI*trun(n);
RTYI(n) = RY0;
RT(n) = sqrt(RTXI(n).^2+RTYI(n).^2);
RMTX(n) = RTXI(n)-RMXI(n);
RMTY(n) = RTYI(n)-RMYI(n);
RMT(n) = sqrt(RMTX(n).^2+RMTY(n).^2);
[mtbx(n),mtby(n)] = i2btran(RMTX(n),RMTY(n),I2B);
psilos(n) = atan2(mtby(n),mtbx(n));
psilosd(n) = psilos(n)*r2d;
RCSt(n) = raylei(psilos(n));

% Missile/Target/Decoy Relative Geometry
RDXI(n) = RTXI(n)+TDXI;
RDYI(n) = RTYI(n)+TDYI;
MDXI(n) = RDXI(n)-RMXI(n);
MDYI(n) = RDYI(n)-RMYI(n);
RMD(n) = sqrt(MDXI(n).^2+MDYI(n).^2); [
mdbx(n),mdby(n)] = i2btran(MDXI(n),MDYI(n),I2B);
psid(n) = atan2(mdby(n),mdbx(n));
psidd(n) = psid(n)*r2d;
disc(n) = max(RMT(n),RMD(n));
RXI(n) = RMTX(n)+.5.*TDXI;
RYI(n) = RMTY(n)+.5.*TDYI;
RR(n) = sqrt(RXI(n).^2+RYI(n).^2);
subang(n) = acos( (RMT(n).^2+RMD(n).^2-TL^2)./(2*RMT(n)*RMD(n)) );
dL(n) = RMD(n)-RMT(n).*cos(subang1(n));
dphase(n) = rem(4.*pi.*dL(n)./(.03),2*pi);    % Wavelength = 0.03m
VMTX(n) = VTXI-VMXI(n);
VMTY(n) = VTYI-VMYI(n);

% End Game Condition
if ((RMT(n) <= md) | (RMD(n) <= md))
        MD1 = RMT(n)
        MD2 = RMD(n)
```

```
            TIME = trun(n) break          % end md requirement
end
end
end      % end while
min(RMT)
min(RMD)
```

APPENDIX B - SEEKER MODEL

```
[skrang,skrd,VE,Vsum,Vdel,Pest]=yskr(psit,oldang,rold,flag,step,RCSt,RCSd,...
                subang,dphase,psid)
r2d = 180/pi;
d2r = pi/180;
bw = .03/.15;
sq = bw/3;

% Realtive to Seeker's Tracking Axis
psi1 = psit-oldang;

% Target Contributions
pa1 = psi1-sq;
S1 = RCSt.*exp(-2.76.*(pa1./bw).^2);
pa2 = psi1+sq;
S2 = RCSt.*exp(-2.76.*(pa2./bw).^2);

% Realtive to Seeker's Tracking Axis
psi2 = psid-oldang;

% Decoy Contributions
pb1 = psi2-sq;
J1 = RCSd.*exp(-2.76.*(pb1./bw).^2).*exp(j.*dphase);
pb2 = psi2+sq;
J2 = RCSd.*exp(-2.76.*(pb2./bw).^2).*exp(j.*dphase);

% Antenna Ouput Voltages
V1 = S1+J1;
V2 = S2+J2;
Vsum = V1+V2;
Vdel = V1-V2;

% Error Voltage
VE1 = real(Vdel./Vsum);

if (abs(VE1)) >= 1
        VE = 0.9987*sign(VE1);
else
```

```
        VE = VE1;
end

% Angle Estimation
temp = 3*bw.*(log(1+VE)-log(1-VE));
Pest = temp./(4*2.76);

% Seeker Angle Servo
w = 2*pi*20;
s = exp(-w*step);
skrd = VE*Pest+rold.*s;
skrang1 = oldang+Pest;

% Angle Limiter
if (abs(skrang1)) > 45*d2r
        skrang = 45*d2r*sign(skrang1);
else
        skrang = skrang1;
end
```

LIST OF REFERENCES

1. Knott, E. F., Shaeffer,J. F., and Tuley, M. T., "Radar Cross Section, 2nd ed.", Artech House Inc., 1993.

2. Stephen M. Hardy, "The Art of Seduction", *Journal of Electronic Defense*, Dec., 1994.

BIBLIOGRAPHY

1. Eichblatt et al, "Test and Evaluation of The Tactical Missiles", Vol. 119, Progress in Astronautics and Aeronautics, AIAA, Inc., 1989.

2. Garnell, P., "Guided Weapon Control Systems", 2nd ed., Pergamon Press., 1980.

3. Golden, August, "Radar Electronic Warfare", AIAA, Inc., 1987.

4. Locke, A. S., "Principles of Guided Missile Design", D. Van Nostrand Co., 1955.

5. Menegozzi, L. and High, W., "Towed-Decoy Effectiveness: A Kinematics Model," *Journal of Electronic Defense*, Apr., 1990.

6. S. M. Sherman, "Monopulse Principles and Techniques", Artech House, Inc., 1984.

7. M. I. Skolnik, "Introduction to Radar Systems, 2nd ed.", McGraw-Hill, Inc., 1980.

INITIAL DISTRIBUTION LIST

1. Defense Technical Information Center   2
   Cameron Station
   Alexandria, VA 22304-6145

2. Library, Code 52   2
   Naval Postgraduate School
   Monterey, CA 93943-5101

3. Department Chairman, Code 37   1
   Naval Postgraduate School
   Monterey, CA 93943

4. D. C. Schleher, Code EW/Sc   3
   Department of Electrical and Computer Engineering
   Naval Postgraduate School
   Monterey, CA 93943

5. David Jenn, Code EC/ Jn   1
   Department of Electrical and Computer Engineering
   Naval Postgraduate School
   Monterey, CA 93943

6. Chung-Shan Institute of Science and Technology   3
   P. O. Box # 90008-6-14, Lung-Tang,
   Tao-Yuan, Taiwan, R. O. C.

7. Jia-Hsin,Yeh   2
   CAPT, Taiwan Air Force, R. O. C.
   4F, #8-2, Chin-Yun Rd., Tu-Cheng, Taipei, Taiwan, R. O. C.